Jefferson.

Thomas Jefferson University
Jefferson Digital Commons

Department of Cancer Biology Faculty Papers | Department of Cancer Biology

9-1-2015

ErbB3-ErbB2 Complexes as a Therapeutic Target in a Subset of Wild-type BRAF/NRAS Cutaneous Melanomas.

Claudia Capparelli
Thomas Jefferson University, Claudia.Capparelli@jefferson.edu

Sheera Rosenbaum
Thomas Jefferson University, sheera.rosenbaum@jefferson.edu

Lisa D. Berman-Booty
Thomas Jefferson University, Lisa.Berman-Booty@jefferson.edu

Amel Salhi
NewYork University School of Medicine

Nadège Gaborit
Weizmann Institute of Science

See next page for additional authors

Let us know how access to this document benefits you

Follow this and additional works at: https://jdc.jefferson.edu/cbfp

 Part of the Oncology Commons

Recommended Citation
Capparelli, Claudia; Rosenbaum, Sheera; Berman-Booty, Lisa D.; Salhi, Amel; Gaborit, Nadège; Zhan, Tingting; Chervoneva, Inna; Roszik, Jason; Woodman, Scott E.; Davies, Michael A.; Setiady, Yulius Y.; Osman, Iman; Yarden, Yosef; and Aplin, Andrew E., "ErbB3-ErbB2 Complexes as a Therapeutic Target in a Subset of Wild-type BRAF/NRAS Cutaneous Melanomas." (2015). *Department of Cancer Biology Faculty Papers.* Paper 98.
https://jdc.jefferson.edu/cbfp/98

This Article is brought to you for free and open access by the Jefferson Digital Commons. The Jefferson Digital Commons is a service of Thomas Jefferson University's Center for Teaching and Learning (CTL). The Commons is a showcase for Jefferson books and journals, peer-reviewed scholarly publications, unique historical collections from the University archives, and teaching tools. The Jefferson Digital Commons allows researchers and interested readers anywhere in the world to learn about and keep up to date with Jefferson scholarship. This article has been accepted for inclusion in

Authors
Claudia Capparelli, Sheera Rosenbaum, Lisa D. Berman-Booty, Amel Salhi, Nadège Gaborit, Tingting Zhan, Inna Chervoneva, Jason Roszik, Scott E. Woodman, Michael A. Davies, Yulius Y. Setiady, Iman Osman, Yosef Yarden, and Andrew E. Aplin

This article is available at Jefferson Digital Commons: https://jdc.jefferson.edu/cbfp/98

Author Manuscript

Author Manuscript

Author Manuscript

Author Manuscript

HHS Public Access

Author manuscript

Cancer Res. Author manuscript; available in PMC 2016 September 01.

Published in final edited form as:

Cancer Res. 2015 September 1; 75(17): 3554–3567. doi:10.1158/0008-5472.CAN-14-2959.

ErbB3/ErbB2 complexes as a therapeutic target in a subset of wild-type BRAF/NRAS cutaneous melanomas

Claudia Capparelli[1], **Sheera Rosenbaum**[1], **Lisa D. Berman-Booty**[1], **Amel Salhi**[2], **Nadège Gaborit**[3], **Tingting Zhan**[4], **Inna Chervoneva**[4], **Jason Roszik**[5,6], **Scott E. Woodman**[5,6], **Michael A. Davies**[5], **Yulius Y. Setiady**[7], **Iman Osman**[2,8], **Yosef Yarden**[3], and **Andrew E. Aplin**[1]

[1]Department of Cancer Biology, Sidney Kimmel Cancer Center, Thomas Jefferson University, Philadelphia, PA 19107, USA

[2]The Ronald O. Perelman Department of Dermatology, New York University School of Medicine, New York, NY 10016, USA

[3]Department of Biological Regulation, Weizmann Institute of Science, Rehovot, Israel

[4]Division of Biostatistics, Department of Pharmacology and Experimental Therapeutics, Thomas Jefferson University, Philadelphia, PA 19107, USA

[5]Department of Melanoma Medical Oncology, The University of Texas MD Anderson Cancer Center, Houston, TX 77054, USA

[6]Department of Systems Biology, The University of Texas MD Anderson Cancer Center, Houston, TX 77054, USA

[7]ImmunoGen, Inc., Waltham, MA 02451, USA

[8]The Interdisciplinary Melanoma Cooperative Group, New York University School of Medicine, New York, NY 10016, USA

Abstract

The treatment options remain limited for melanoma patients who are wild-type for both BRAF and NRAS (WT/WT). We demonstrate that a subgroup of WT/WT melanomas display high basal phosphorylation of ErbB3 that is associated with autocrine production of the ErbB3 ligand, neuregulin-1 (NRG1). In WT/WT melanoma cells displaying high levels of phospho-ErbB3, knockdown of NRG1 reduced cell viability and was associated with decreased phosphorylation of ErbB3, its co-receptor ErbB2 and its downstream target, AKT. Similar effects were observed by targeting ErbB3 with either small interfering RNAs or the neutralizing ErbB3 monoclonal antibodies, huHER3-8 and NG33. Additionally, pertuzumab-mediated inhibition of ErbB2 heterodimerization decreased AKT phosphorylation, cell growth *in vitro* and xenograft growth *in*

Corresponding author: Andrew E. Aplin, Department of Cancer Biology, Thomas Jefferson University, 233 South 10th Street, Philadelphia, PA 19107. Tel: (215) 503-7296. Fax: (215) 923-9248; aea004@jefferson.edu.
The current address for L.D. B-B is Bristol-Myers Squibb, PO Box 5400, Princeton, NJ 08543, USA.

Disclosure of potential conflicts of interest: M.A.D. has received research grants from GlaxoSmithKline, Genentech, AstraZeneca, Oncothyreon Merck and Sanofi Aventis and serves as a consultant for GlaxoSmithKline, Genentech, Novartis and Sanofi Aventis. All other authors declare they have no competing financial relationships.

Author Manuscript Author Manuscript Author Manuscript Author Manuscript

vivo. Pertuzumab also potentiated the effects of MEK inhibitor on WT/WT melanoma growth *in vitro* and *in vivo.* These findings demonstrate that targeting ErbB3-ErbB2 signaling in a cohort of WT/WT melanomas leads to tumor growth reduction. Together these studies support the rationale to target the NRG1-ErbB3-ErbB2 axis as a novel treatment strategy in a subset of cutaneous melanomas.

Keywords

ErbB3; HER3; ErbB2; pertuzumab

Introduction

There have been remarkable advances in the targeted therapy options for cutaneous melanoma. Since 2011, the BRAF inhibitors vemurafenib and dabrafenib, the MEK inhibitor trametinib, and the dabrafenib plus trametinib combination have all been approved by the FDA for V600E mutant BRAF-harboring melanoma patients based on their high clinical response rates, prolonged progression-free survival and improved overall survival compared to chemotherapy (1-4). While mutant BRAF tumors make up approximately 50% of cutaneous melanomas, distinct subsets harbor NRAS mutations (~15%) or are wild-type for both BRAF and NRAS (WT/WT) (~35%). In non-V600E BRAF melanoma, there is lack of effective targeted therapy options. While immune checkpoint inhibitors, which act in a genotype-independent manner, have recently gained FDA-approval (5, 6), additional therapeutic treatment options are needed. Studies have sought to identify other driver mutations in addition to the known alterations in BRAF and NRAS (7, 8) especially given that melanomas derived from sun-exposed regions that are WT/WT exhibit high mutation counts and UV damage signatures (8, 9). Somatic mutations in the *KIT*, *NF1*, and *NOTCH1* genes have been identified in WT/WT melanomas but non-mutational alterations are also likely to be important (7, 8, 10).

ErbB3/HER3 (v-erb-b2 erythroblastic leukemia viral oncogene homolog 3/human epidermal receptor 3) is a member of the EGF family of cell surface receptors. Compared to the other members (EGFR/ErbB1, ErbB2 and ErbB4), ErbB3 exhibits low kinase activity but remains an effective mediator of signal transduction (11, 12). Following binding of its ligand, neuregulin-1 (NRG1), ErbB3 does not regularly form homodimers but pairs with other EGFR family members (13); the ErbB3-ErbB2 heterodimer being the most potent pairing (14-16). The cytoplasmic tail of ErbB3 contains multiple tyrosine residues, which are phosphorylated by its co-receptor following NRG1-binding and serve as docking sites for adaptors leading to the activation of the PI-3 kinase-AKT and MEK-ERK1/2 signaling pathways (16). Elevated expression of NRG1 and functional NRG1/ErbB3 autocrine loops have been associated with tumor progression in models of head and neck squamous cell carcinoma (17) and ovarian cancer (18).

Activation of ErbB3 is related to the progression of several cancer types (19). NRG1-ErbB3 signaling plays an important role in melanocyte homeostasis (20) and high ErbB3 expression was detected in 40% (35 out of 87) of melanoma patients and is associated with

Author Manuscript Author Manuscript Author Manuscript Author Manuscript

poor prognosis (21). Proteomic studies indicate that ErbB3 is highly phosphorylated in some melanoma cell lines (22). In mutant BRAF melanomas, ErbB3 expression and ligand-stimulated phosphorylation are up-regulated by BRAF inhibitors, such as vemurafenib, as part of an adaptive compensatory mechanism (23). Due to the unmet clinical need for targeted therapy options in WT/WT melanoma, we examined phosphorylation of ErbB3 in this subset of melanoma. We show high levels of phosphorylated ErbB3 and its co-receptor ErbB2 in a subset of WT/WT melanomas. In this subset, depletion of NRG1 or ErbB3 led to inhibition of downstream AKT phosphorylation and cell growth. Similarly, antibody-mediated targeting of the ErbB3-ErbB2 axis impaired the growth of WT/WT melanomas *in vitro* and *in vivo* and potentiated the effects of a MEK inhibitor. These preclinical data suggest that targeting the NRG1-ErbB3-ErbB2 axis may serve as a treatment strategy in a subset of WT/WT melanomas.

Materials and Methods

Cell culture

The human melanoma cell lines CHL-1, SKMEL2 and A375 were purchased from ATCC (Manassas, VA). WM3928 cells were purchased from the Coriell Institute (Camden, NJ). The following cell lines were kindly donated: Bowes (Dr. Mark Bracke, University Hospital, Ghent, Belgium); YUHEF and YUROL (Dr. Ruth Halaban, Yale University, New Haven, CT) and CCMMATI (ATI), FEMX, MEWO and CCMMB6 (B6) (Dr. Barbara Bedogni, Western Reserve University, Cleveland, OH); SK-MEL173 (Dr. David Solit Memorial Sloan Kettering, NY); WM1346, WM1361A, WM1366, WM3912, WM3211, WM266-4, WM239-A, and WM115 (Dr. Meenhard Herlyn, Wistar Institute, Philadelphia, PA). Cell lines were sequenced in both directions for BRAF and NRAS mutations (Supplemental Fig. 1A). STR analysis was completed for cell lines in January 2015, confirming that A375, CHL-1, MEWO, WM3912, WM3928, WM239-A, WM266-4, WM115, WM1366, SKMEL-2, and Bowes match known profiles, and FEMX, YUROL, SKMEL-173, B6, ATI and YUHEF have unique profiles. Cell lines were cultured as follows: CHL-1, ATI, FEMX, MEWO and B6 (DMEM supplemented with 10% FBS); Bowes (MEM with 10% FBS and non-essential amino acids); YUHEF (Opti-MEM containing 5% FBS); WM1346, WM1361A, WM1366, WM3912, WM3211 and WM3928 (MCDB 153 with 2% FBS, 20% Leibovitz L-15 medium, 5 μg/ml insulin); SKMEL2 (MEM supplemented with 10% FBS) and SKMEL173 (RPMI with 10% FBS). Cells were used at low passages from purchase/donation.

Human metastatic melanoma tumors collection

All tissue specimens from the NYU melanoma clinicopathological biospecimen database (24) have been histologically confirmed by a pathologist and have previously been screened for mutations in BRAF and NRAS genes. Tumors from WT/WT melanoma patients were microdissected and were harvested in extraction buffer.

Growth factors and anti-ErbB antibodies

Recombinant human NRG1 was purchased from Cell Signaling Technology (Danvers, MA). Pertuzumab was obtained from the Thomas Jefferson University Pharmacy. huHER3-8, an

Author Manuscript Author Manuscript Author Manuscript Author Manuscript

ErbB3 antagonistic humanized antibody (22), was produced and purified at ImmunoGen, Inc. The monoclonal antibody, NG33, blocks NRG1 binding to the ErbB3 (25). Trametinib/GSK'212 and PD0325901 were purchased from Selleck Chemicals LLC (Houston, TX).

Short-interfering RNA (siRNA) and transfection

Cells were transfected with chemically synthesized siRNAs (Dharmacon Inc., LaFayette, CO) at a final concentration of 25 nM using Lipofectamine RNAiMAX (Invitrogen, Carlsbad, CA). Sequences used were: CTL, UGGUUUACAUGUCGACUAA; NRG1$^{\#02}$ is a Smartpool of 4 sequences; NRG1$^{\#21}$, UUUCAAACCCCUCGAGAUA; NRG1$^{\#09}$ is an on-target modified form of NRG1$^{\#21}$; ErbB3$^{\#08}$, GCAGUGGAUUCGAGAAGUG; ErbB3$^{\#22}$, AGAUUGUGCUCACGGGACA; ErbB2$^{\#04}$ is a Smartpool of 4 sequences.

Reverse Phase Protein Array (RPPA)

RPPA was performed across a panel of patient samples from The Cancer Genome Atlas (TCGA; https://tcga-data.nci.nih.gov/tcga/), as previously described (26-28). Results were normalized across the entire panel of antibodies and, for pErbB3 representation, the data were normalized for the median of pErbB3 values across all genotypes and log2 transformed.

Western blotting

Cells were washed twice in cold PBS and lysed with Laemmeli sample buffer. Lysates were resolved by SDS polyacrylamide gel electrophoresis and transferred to PVDF membranes. For secreted NRG1 detection, medium was collected and centrifuged for 30 mins at 4000 rpm in an Amicon ultra conical tube. Laemmeli sample buffer was added and samples resolved by SDS-PAGE. After blocking in 5% BSA, membranes were incubated with the indicated primary antibodies overnight at 4 °C, followed by incubation with peroxidase-coupled secondary antibodies. Bound antibodies were detected using enhanced chemiluminescence substrate (Pierce, Rockford IL). Chemiluminescence was visualized on a VersaDoc Multi-Imager and quantitated using Quantity-One software (BioRad, Hercules, CA). Primary antibodies used were: NRG1 (# MAB377) antibody purchased from R&D Biosystems (Minneapolis, MN) used for detection of secreted NRG1, ERK2 (sc-1647) and EGFR (sc-03) antibodies purchased from Santa Cruz Biotechnology Inc. (Santa Cruz, CA); NRG1 (#2573), p-ErbB3 (Y1197, #4561), ErbB3 (#4754), p-ErbB2 (Y1196, #6942), ErbB2 (#4290), p-AKT (S473, #6942), p-AKT (T308, #2965), AKT (#9272) and p-ERK1/2 (T202/Y204, #9101) purchased from Cell Signaling Technology; actin (A2066) antibody purchased from Sigma-Aldrich Co. (St. Louis, MO).

5-ethynyl-2'-deoxyuridine (EdU) incorporation assays

siRNA-transfected cells (72 hr post-transfection) were incubated with EdU for 5 hr. Then, cells were trypsinized, washed twice with PBS containing 1% BSA and processed according to the manufacturer's instruction using the Alexa Fluor 647 Flow Cytometry Assay Kit (Invitrogen). Samples were analyzed using the FACS Calibur Flow Cytometer.

Author Manuscript Author Manuscript Author Manuscript Author Manuscript

Annexin V staining

Cells were transfected with siRNAs, as described above. After 72 hr, cells were replated in 3D collagen gels as described (29) for further 48 hr. Then, cells were collected and incubated with annexin V-APC (BD Biosciences, San Jose, CA) and propidium iodide for 30 min at room temperature. Samples were analyzed using the FACS Calibur Flow Cytometer.

Cell growth assays

Cells were plated at low density in individual wells of 6-well plates and treated, as indicated. Cells were then washed with PBS and stained with crystal violet solution (0.2% crystal violet in 10% buffered formalin) for 20 min. Subsequently, wells were washed and air-dried. Plates were scanned and quantitative analysis was performed using Image J software. Pictures were taken with Nikon Eclipse Ti inverted microscope with NIS-Elements AR 3.00 software (Nikon, Melville, NY).

In vivo xenograft experiments

The animal experiments were performed in a facility at Thomas Jefferson University that is accredited by the Association for the Assessment and Accreditation of Laboratory Animal Care (AAALAC). Studies were approved by the Institutional Animal Care and Use Committee (IACUC). CHL-1 (5×10^6) or Bowes (4×10^6) cells were injected intradermally into the back of female athymic mice in 100 μl of PBS. When tumors were palpable, mice were divided in 2 groups for either vehicle (PBS) or pertuzumab (2 mg/ml; 200 μg/mouse) treatment. For the combination treatment experiment, mice were divided into 4 groups: vehicle, pertuzumab alone, MEK inhibitor alone (PD0325901, chow 7 mg/kg), and pertuzumab in combination with PD0325901. Pertuzumab was administered intraperitoneally every 3 days in 100 μl of PBS. Measurements of tumor size were taken every 3 days using digital calipers, and tumor volume was determined by the following formula: volume = (length × width^2) × 0.52.

Immunohistochemistry

Tumors from CHL-1 intradermal xenografts were harvested, fixed in formalin and paraffin-embedded. Seven control and six pertuzumab-treated xenografts were immunostained with Ki67 antibody (Thermo Fisher Scientific, Tewksbury, MA). Three random images from each slide were obtained at 400× magnification. The manual cell counter feature of the ImageJ64 (National Institutes of Health, Bethesda, MD) image analysis software was used to quantify positive and negative cells. GraphPad Prism was employed to perform statistical analysis. Sections from 3 control xenografts and 3 xenografts treated with pertuzumab were immunostained for pS473 AKT (Cell Signaling Tech., #6942) and percentage of cells that were immunopositive as well as the relative intensities were determined in a sample blinded manner.

Statistical analysis

Statistical analysis for EdU staining, annexin V and crystal violet quantification and tumor volume comparison was performed using student t-test two-tailed, unpaired, assuming

Author Manuscript Author Manuscript Author Manuscript Author Manuscript

unequal variance. The Spearman correlation coefficient was used to compare pErbB3, and NRG1 expression levels in melanoma samples from TCGA. For *in vivo* experiment data, log-transformed tumor volumes were analyzed using linear mixed (LME) models with fixed effects of treatment group, post-treatment days, and their interaction and random effects of animal in the slope and intercepts of the animal-specific growth curves. The fitted LME model was used to compare mean tumor volumes between treatment and control groups at each time point between 0 and 24 (pertuzumab alone) or 27 (combination) days for CHL-1 injected mice and between 0 and 21 days for Bowes injected mice.

Results

ErbB3 is highly phosphorylated in a subset of WT/WT melanoma cell lines

To investigate the role of NRG1-ErbB3 pathway in WT/WT melanoma, we examined reverse phase protein array (RPPA) data from The Cancer Genome Atlas (TCGA; https://tcga-data.nci.nih.gov/tcga/) stratified for different genetic subclasses of melanomas. A range of phospho-ErbB3 levels were detected in WT/WT melanomas (Fig. 1A). A similar heterogeneity was observed in other genotypic subgroups: V600E/K BRAF; other BRAF mutations; mutant NRAS. Since NRG1, the ligand for ErbB3, may be derived from either tumor or stromal cells, we examined levels of NRG1 and ErbB family receptors (EGFR, ErbB2, ErbB3 and ErbB4) in melanoma cell monocultures by Western blot. NRG1 and ErbB3 were both expressed and phospho-ErbB3 was readily detectable in a subset of WT/WT cell lines, suggesting an autocrine NRG1/ErbB3 loop in these cells (Fig. 1B, 1C). Phospho-ErbB3 levels were particularly high in CHL-1 and Bowes cells, intermediate in YUHEF and ATI cells, but low in YUROL and WM3211 and five other WT/WT lines (Supplemental Fig. 1B). In the 4 mutant BRAF and 4 mutant NRAS melanoma cell lines tested, we did not detect high phospho-ErbB3 levels due to mutually exclusive expression of NRG1 and ErbB3 (Fig. 1C). Consistent with protein data, mRNA levels of NRG1 were high in CHL-1 and Bowes cells and intermediate in YUHEF and ATI cells (Supplemental Fig. S1C). ErbB4 expression was not detected in any of the cell lines analyzed (Supplemental Fig. S1D).

The lack of targeted inhibitor strategies for WT/WT melanoma patients is a clinically unmet need and a subset of WT/WT melanoma display an autocrine NRG1/ErbB3 loop; hence, we decided to focus on this subgroup. To confirm that ErbB3 is hyper-activated in WT/WT melanoma, we analyzed NRG1 and ErbB3 phosphorylation levels in a cohort of WT/WT human melanoma tissues. In contrast to human melanocytes (HEM-377 and HEM-475), 6 out of 9 (67%) human metastatic WT/WT melanoma displayed highly phosphorylated ErbB3 that was associated with NRG1 expression (Fig. 1D). The relevance of the NRG1/ErbB3 pathway in WT/WT melanoma was further supported by the statistical analysis of the TCGA RPPA dataset. Spearman correlation coefficient showed a significant positive correlation between NRG1 and pErbB3 expression in WT/WT melanoma (Supplemental Fig. S1E). We do not rule out the possibility that subsets of the mutant NRAS and mutant BRAF melanoma cohorts may also co-express NRG1 and ErbB3. In addition, pErbB3 and NRG1 were co-expressed in 13 out of 42 (31%) of WT/WT patients in the TCGA RPPA

Author Manuscript Author Manuscript Author Manuscript Author Manuscript

dataset (Fig. 1E). Overall, these findings suggest that ErbB3 signaling is activated by autocrine production of NRG1 in a subset of WT/WT cutaneous melanomas.

NRG1 is required for cell growth and survival in WT/WT melanoma cell lines

We further studied the role of NRG1 in WT/WT melanoma cell lines. First, we established that CHL-1, Bowes and YUHEF cell lines express and secrete NRG1 into the conditioned medium (Fig. 2A). NRG1 knockdown using multiple siRNAs reduced NRG1 secretion and levels of phosphorylated ErbB3, ErbB2, AKT and ERK1/2 (Fig. 2B & Supplemental Fig. S2A, S2B). NRG1 knockdown elicited either minor or no effect on STAT3 phosphorylation (Supplemental Fig. S2B). Addition of exogenous NRG1 rescued the effects of silencing, confirming that effects were specific to NRG1 knockdown. The reduction of ErbB3 expression following NRG1 knockdown in some cell lines is likely due to the reduced stability of the receptor in the absence of the ligand and was not detected at early time points in knockdown experiments (Supplemental Fig. S2C).

We investigated the functional role of NRG1 in melanoma cells by EdU incorporation and annexin V staining assays to measure S phase entry and apoptosis, respectively. The depletion of NRG1 in CHL-1 and Bowes cells reduced EdU incorporation (Fig. 2C) and increased annexin V staining (Fig. 2D); effects that were reversed by addition of exogenous NRG1. The increased apoptosis was associated with up-regulation of the pro-apoptotic BH3-only protein, BIM-EL, but no alterations in the expression of the pro-survival protein, MCL-1 were detected (Supplemental Fig. S2D). Next, we evaluated the effects of NRG1 knockdown on cell growth in WT/WT melanoma cells. The efficiency of the NRG1 knockdown throughout the duration of the growth assay (7 days) was validated (Supplemental Fig. S2E). NRG1 depletion dramatically reduced the growth of CHL-1, Bowes, YUHEF and ATI cells, effects that were rescued by addition of exogenous NRG1 (Fig. 2E & Supplemental Fig. S2F). NRG1 depletion in NRG1-epxressing mutant NRAS melanoma cell lines, WM1346, WM1361A and WM1366, did not alter AKT phosphorylation, EdU incorporation or cell growth (Supplemental Fig. S2G, S2H & S2I), likely due to the low/undetectable levels of ErbB3 in these cells (Fig. 1B). Together, these data indicate that NRG1 regulates cell growth and apoptosis in a subset of WT/WT melanoma cell lines that display high levels of phospho-ErbB3.

Depletion of ErbB3 reduces S-phase entry and cell growth and induces apoptosis

NRG1 binds to both ErbB3 and ErbB4 receptors. While mutations in ErbB4 have been identified in melanoma (30), we were unable to detect ErbB4 expression in our cell lines (Supplemental Fig. S1D). Given the changes in phospho-ErbB3 associated with NRG1 knockdown, we tested the requirement of ErbB3 in WT/WT melanoma by siRNA-mediated depletion. Similar to effects with NRG1 depletion, ErbB3 knockdown with two independent siRNAs reduced the phosphorylation of ErbB2, AKT and ERK1/2 in CHL-1 and Bowes cells (Fig. 3A and Supplemental Fig. S3A). Depletion of ErbB3 was also associated with reduced S-phase entry and enhanced apoptosis in both cell lines (Fig. 3B & 3C). Finally, knockdown of ErbB3 in CHL-1 and Bowes cells plated at clonal density significantly reduced cell growth (Fig. 3D). These data show that in phospho-ErbB3 high WT/WT melanoma, ErbB3 is required for growth and survival.

Author Manuscript Author Manuscript Author Manuscript Author Manuscript

Targeting ErbB3 with neutralizing antibodies reduces phosphorylation of AKT and ERK1/2 and inhibits cell growth

Since our results suggest that inhibiting NRG1 and ErbB3 signaling is a rational therapeutic strategy in WT/WT melanoma cells showing evidence of pathway activation, we tested the effects of two ErbB3 targeting monoclonal antibodies, NG33 and huHER3-8. NG33 is a monoclonal antibody that blocks the binding of NRG1 to the ErbB3 receptor (25). huHER3-8 is a high affinity, antagonistic anti-ErbB3 antibody that binds within residues 20 and 342 of ErbB3 and out-competes NRG1 binding (31). Treatment of WT/WT melanoma cell lines with either NG33 or huHER3-8 reduced phospho-ErbB3 and phospho-ErbB2 (Fig. 4A & 4B). Furthermore, treatment with either antibody also reduced AKT and ERK1/2 phosphorylation (Fig. 4A, 4B & Supplemental Fig. S4). Although AKT reactivation was noted at later time points, levels remained reduced 70% compared to the untreated conditions throughout the 48 hr treatment (Supplemental Fig. S4). ErbB3 neutralization also inhibited the expression and hyper-phosphorylation of the G1/S phase markers, cyclin A2 and Rb, respectively (Fig. 4C). Furthermore, NG33 and huHER3-8 reduced growth of CHL-1 and Bowes cells (Fig. 4D). As a control, no effect was observed following huHER3-8 treatment in the ErbB3-deficient, mutant NRAS cell lines, WM1346 and WM1361A (Fig. 4E). These data show that targeting an autocrine NRG1-ErbB3 pathway with neutralizing antibodies reduces growth of WT/WT melanoma cells.

Inhibition of ErbB2-ErbB3 dimerization with pertuzumab decreases AKT and ERK1/2 phosphorylation and cell growth *in vitro* and *in vivo*

ErbB3 is a catalytically impaired member of the ErbB family and partners with other ErbB family members in response to NRG1 binding (32). Our results show that NRG1 knockdown and ErbB3 targeting decreased phospho-ErbB2 levels. To determine whether ErbB2 is required for phospho-ErbB3 levels in WT/WT melanoma cells, CHL-1 cells were depleted of ErbB2. Knockdown of ErbB2 abolished phosphorylation of ErbB3, AKT and ERK1/2 (Fig. 5A). Additionally, treatment of CHL-1, Bowes and ATI cells with pertuzumab, a clinical grade antibody that inhibits ErbB2-ErbB3 dimerization, effectively reduced the levels of ErbB3, AKT and ERK1/2 phosphorylation at all doses and times analyzed (Fig. 5B & Supplemental Fig. S5A & S5B). Notably, pertuzumab did not alter AKT or ERK1/2 phosphorylation in the ErbB3-deficient, mutant NRAS cell lines, WM1361-A and WM1366 (Supplemental Fig. S5C). These data indicate that ErbB2 is required for ErbB3 activation in WT/WT melanoma cells displaying high phospho-ErbB3.

Next, we tested the effects of pertuzumab on WT/WT melanoma cell growth *in vitro* and *in vivo*. Similar to effects with huHER3-8, pertuzumab reduced cyclin A expression and Rb hyper-phosphorylation in CHL-1 and Bowes cells (Fig. 5C). In *in vitro*colony growth assays, pertuzumab significantly inhibited the growth of CHL-1, Bowes and ATI at all doses indicated (Fig. 5D & Supplemental Fig. S5D). WT/WT cell lines with low NRG1 expression did not show dependency on this pathway (Supplemental Fig. S5E). Similar to huHER3-8, pertuzumab did not induce any effect on cell growth in the mutant NRAS cell lines analyzed, WM1346, WM1361A, SKMEL2 and SKMEL173 (Fig. 5E & Supplemental Fig. S5F). For *in vivo* analysis, CHL-1 and Bowes cells were injected intradermally in athymic mice. Palpable xenograft tumors were treated with either vehicle or pertuzumab every 3

Author Manuscript Author Manuscript Author Manuscript Author Manuscript

days. Compared to control tumors, we observed a dramatic reduction in tumor growth in pertuzumab-treated mice (Fig. 6A & 6B). This effect was evident and statistically significant as early as day 6 and day 3 following treatment with pertuzumab for CHL-1 and Bowes xenografts, respectively. Reduced tumor growth was associated with reduction in phospho-AKT staining (Fig. 6C) and a statistically significant reduction in Ki67 staining in tumors treated with pertuzumab compared to the control tumors (Fig. 6D).

To investigate if the reduction of AKT phosphorylation is a major mechanism of pertuzumab action, we used the AKT inhibitor, MK2206. Consistently, we observed a dose-dependent reduction of AKT phosphorylation associated with reduction of cell growth (Supplemental Fig. S5G & S5H). Due to the stronger effects observed following pertuzumab treatment, we do not rule out the possibility that ErbB3 also acts through AKT-independent mechanisms (33). Since we detected a partial reactivation of AKT signaling following ErbB3/2 antibody treatment, we tested pertuzumab in combination with the AKT inhibitor, MK2206. While we observed reduced cell growth with the combination, only a very modest increase in apoptosis was observed (Supplemental Fig. S5I and Fig. S5L). These data are consistent with the *in vitro* ErbB3-ErbB2 targeting data and indicate that WT/WT melanomas exhibiting high levels of phospho-ErbB3 may be treatable with an FDA-approved agent.

MEK inhibition potentiates the effects of pertuzumab on cell growth *in vitro* and *in vivo*

Due to the frequent dependence of melanomas on the ERK1/2 pathway, we considered the effects of the combination of pertuzumab with the MEK inhibitor, GSK'212 (trametinib), in this subgroup of WT/WT cell lines. With GSK'212 treatment alone, we observed a dose-dependent growth reduction in CHL-1 and Bowes cells that was associated with decreased ERK1/2 phosphorylation (Fig. 7A). The combined treatment of pertuzumab with GSK'212 significantly potentiated the effect, resulting in a significant reduction in cell growth in CHL-1 and Bowes cells compared to each single agent *in vitro* (Fig. 7B). *In vivo*, the combined action of pertuzumab and MEK inhibitor (PD0325901) significantly reduced CHL-1 xenograft growth compared to either MEK inhibitor alone or pertuzumab alone (Fig. 7C and Supplemental Fig. S6). These data indicate that MEK inhibitors may enhance the effects of targeting the ErbB3/2 pathway in NRG1-expressing WT/WT melanomas.

Discussion

Emerging data suggest a role for the growth factor receptor ErbB3 in promoting tumorigenesis and mediating compensatory signaling in response to targeted inhibitors. Despite evidence for an important developmental role of ErbB3 in the melanocytic lineage, its function in cutaneous melanoma has been unclear. Phospho-ErbB3 levels in patient samples were heterogeneous in the three main genetic subgroups of melanoma: mutant BRAF, mutant NRAS, and WT for both BRAF and NRAS. We have previously shown that in mutant BRAF melanomas, baseline ErbB3 signaling does not dramatically effect tumor growth but it is up-regulated in response to BRAF inhibitors such as vemurafenib and mediates adaptive resistance (23, 34). Furthermore, unphosphorylated ErbB3 was readily detectable in many mutant BRAF lines and is associated with low-undetectable levels of

Author Manuscript Author Manuscript Author Manuscript Author Manuscript

NRG1. In this study, we investigated the role of NRG1/ErbB3 signaling in melanomas that are wild-type for both BRAF and NRAS (WT/WT). We demonstrate that the ligand for ErbB3, NRG1, is highly expressed and activates ErbB3 signaling in an autocrine manner in a subset of WT/WT melanomas. Furthermore, we show that NRG1-ErbB3-ErbB2 signaling is required for malignant traits and inhibition of this signaling axis is a rational therapeutic strategy within this melanoma subset.

Initially, we observed that basal ErbB3 phosphorylation and NRG1 expression are frequently elevated in WT/WT melanomas cell lines and patient samples in the TCGA dataset. Other studies have shown that ErbB3 is highly expressed in 40% (35 out of 87) of melanoma metastases (21) and is associated with a proliferative phenotype in melanoma (35); however, these studies lack genotype stratification. Studies analyzing NRG1 expression in melanoma have provided differing views. While one report showed co-expression of ErbB3 and NRG1 in a subset of human metastatic melanomas (36), another study showed low expression of NRG1 in melanoma cells (37). The high phospho-ErbB3 staining detected in TCGA samples (this study) and in 27% of melanoma metastases (20) likely reflects melanomas that express ErbB3 and either co-express NRG1 or reside in a tumor microenvironment enriched with secreted NRG1. Other WT/WT cell lines showed mutually exclusive expression of NRG1 and ErbB3 indicating the presence of other tumor driving mechanisms and underscoring the need to investigate clinically applicable biomarkers. ErbB3-ErbB2 activation was also detected in some mutant BRAF and mutant NRAS tumors but the presence of a driver mutation may reduce the functional dependency on ErbB3 in this context.

In the present study, we observed that 4 out of 11 WT/WT melanoma cell lines showed dependency on the NRG1 pathway. Given the clinical unmet need for targeted therapies in the WT/WT genotype, we explored the effects of blockade of this pathway in the subset of WT/WT cell lines that express both ErbB3 and NRG1. First, we showed that NRG1 is required for phosphorylation of ErbB3, ErbB2 and AKT. The NRG1 gene generates at least 31 isoforms through alternative promoter usage and splicing (38). In this study, we employed siRNAs that knockdown both α and β isoforms of NRG1. The cytoplasmic tail of ErbB3 harbors six high affinity TxxM binding sites for the p85 regulatory subunit of PI-3 kinase leading to AKT activation (39, 40) and our data are consistent with this pathway being controlled by ErbB3 in WT/WT melanoma. However, we do not exclude that PI-3 kinase signaling may additionally regulate melanoma proliferation through AKT-independent signaling (33). Depleting NRG1 led to decreases in S phase entry, survival in 3D extracellular matrices and cell growth, demonstrating that WT/WT cell lines displaying high levels of phospho-ErbB3 are dependent on autocrine NRG1 signaling. We also directly targeted ErbB3 using either molecular reagents or neutralizing antibodies. Both approaches led to comparable findings to effects seen targeting NRG1, indicating that ErbB3 is the main functional target of NRG1 in these cells. Notably, there are multiple efforts to generate clinical grade ErbB3 neutralizing agents and in this study we utilized two independent antibodies that both inhibit NRG1 binding as well as block ErbB3 dimerization with co-receptors. Other ErbB3 neutralizing antibodies such as U3-1287 (U3-Pharma), MM-121 (Merrimack) and LJM716 (Novartis) are currently being tested in the pre-clinical and clinical settings (41-43). Since our material transfer agreements exclude the comparison of

Author Manuscript Author Manuscript Author Manuscript Author Manuscript

similar antibodies from independent pharmaceutical companies, we were unable to perform side-by-side comparisons of additional antibodies. Notably, in ovarian, breast and lung cancer trials with MM-121, NRG1 mRNA levels were detected by *in situ* hybridization and appear to predict for clinical response (44-46). This raises the possibility of NRG1 RNA levels serving as a biomarker for WT/WT melanomas that will respond to ErbB3 targeting.

Analysis of the co-receptor for ErbB3 also afforded targeting opportunities. ErbB3 is able to partner with multiple co-receptors but primarily utilizes ErbB2 in WT/WT melanoma cells. ErbB2 is the most potent pairing for ErbB3 (14, 15) and is also the preferred partner for ErbB3 in mutant BRAF melanoma cells treated with RAF inhibitors (23). While we did not detect ErbB4 expression in our cell lines, we do not rule out a partial role for ErbB4 in these cells. Pertuzumab, an antibody that binds ErbB2 and targets ErbB2 dimerization with ErbB3, was recently FDA-approved for metastatic breast cancer in combination with trastuzumab and docetaxel (47). The finding that pertuzumab potently blocks signaling and growth of phospho-ErbB3-positive WT/WT melanoma cells both *in vitro* and *in vivo* further highlights the dependency of this sub-group of melanomas on the ErbB3-ErbB2 pathway. These data also provide the basis for exploring pertuzumab as part of a first-line treatment option in WT/WT melanoma patients who display high levels of phospho-ErbB3, phospho-ErbB2 and NRG1. Many current clinical trials utilize anti-ErbB3 targeting agents in combination with chemotherapies and there is a growing awareness that drug combinations are needed in order to obtain durable responses in patients. Since GSK'212/trametinib is FDA-approved for mutant BRAF melanoma, we explored the effects of blocking ErbB3 and MEK in phospho-ErbB3-positive WT/WT melanoma cells. Importantly, the combination of pertuzumab with MEK inhibitor was more effective at blocking growth than either as a single agent *in vitro* and *in vivo*. We did observe tumor regressions with this combination in our *in vivo* study suggesting dependencies on additional pathways and/or the need to examine ways to maximally target the ErbB3 signaling pathway.

In summary, a subgroup of melanoma cell lines and patient samples, which are wild-type for both BRAF and NRAS, display elevated activation of NRG1/ErbB3 pathway. By targeting NRG1, ErbB3 or ErbB2, we demonstrate that this subset of cutaneous melanomas exhibit dependency on this signaling axis. Thus, our study provides pre-clinical evidence for directly targeting ErbB3 and/or ErbB2 in a subset of WT/WT melanomas.

Supplementary Material

Refer to Web version on PubMed Central for supplementary material.

Acknowledgements

We thank Neda Dadpey for performing the DNA sequencing of cell lines, Dr. Michele Weiss for scientific advice, Dr. Marc E. Bracke for the Bowes cells, Dr. Ruth Halaban for the YUHEF cells, Dr. Meenhard Herlyn for the WM cell lines, and Dr. Barbara Bedogni for the ATI, FEMX, MEWO and B6 cells.

Grant Support

This work was supported by grants from OutRun the Sun to C.C., American-Italian Cancer Foundation (AICF) Post-doctoral Research Fellowship to C.C., a NIH K01 award (K01 OD010463) to L.B-B., and from the Dr. Miriam and Sheldon G. Adelson Medical Research Foundation and NIH R01 CA160495 to A.E.A. Additionally, this

Author Manuscript Author Manuscript Author Manuscript Author Manuscript

project was funded, in part, under a grant with the Pennsylvania Department of Health. The Department specifically disclaims responsibility for any analyses, interpretation or conclusion. The TJU SKCC core facilities are funded by a National Cancer Institute (NCI) Support Grant, P30CA56036. The RPPA Core Facility at M.D Anderson is supported by NCI Cancer Center Support Grant, CA-16672.

References

1. Flaherty KT, Robert C, Hersey P, Nathan P, Garbe C, Milhem M, et al. Improved survival with MEK inhibition in BRAF-mutated melanoma. N Engl J Med. 2012; 367:107–14. [PubMed: 22663011]
2. Flaherty KT, Infante JR, Daud A, Gonzalez R, Kefford RF, Sosman J, et al. Combined BRAF and MEK inhibition in melanoma with BRAF V600 mutations. N Engl J Med. 2012; 367:1694–703. [PubMed: 23020132]
3. Das Thakur M, Stuart DD. Molecular pathways: Response and resistance to BRAF and MEK inhibitors in BRAFV600E tumors. Clin Cancer Res. 2013; 20:1074–80. [PubMed: 24352648]
4. Hartsough E, Shao Y, Aplin AE. Resistance to RAF inhibitors revisited. J Invest Dermatol. 2014; 134:319–25. [PubMed: 24108405]
5. Hodi FS, O'Day SJ, McDermott DF, Weber RW, Sosman JA, Haanen JB, et al. Improved survival with Ipilimumab in patients with metastatic melanoma. N Engl J Med. 2010; 363:711–23. [PubMed: 20525992]
6. Hamid O, Robert C, Daud A, Hodi FS, Hwu WJ, Kefford R, et al. Safety and tumor responses with lambrolizumab (anti-PD-1) in melanoma. N Engl J Med. 2013; 369:134–44. [PubMed: 23724846]
7. Hodis E, Watson IR, Kryukov GV, Arold ST, Imielinski M, Theurillat JP, et al. A landscape of driver mutations in melanoma. Cell. 2012; 150:251–63. [PubMed: 22817889]
8. Krauthammer M, Kong Y, Ha BH, Evans P, Bacchiocchi A, McCusker JP, et al. Exome sequencing identifies recurrent somatic RAC1 mutations in melanoma. Nat Genet. 2012; 44:1006–14. [PubMed: 22842228]
9. Mar VJ, Wong SQ, Li J, Scolyer RA, McLean C, Papenfuss AT, et al. BRAF/NRAS wild-type melanomas have a high mutation load correlating with histologic and molecular signatures of UV damage. Clin Cancer Res. 2013; 19:4589–98. [PubMed: 23833303]
10. Nissan MH, Pratilas CA, Jones AM, Ramirez R, Won H, Liu C, et al. Loss of NF1 in cutaneous melanoma is associated with RAS activation and MEK dependence. Cancer Res. 2014; 74:2340–50. [PubMed: 24576830]
11. Guy PM, Platko JV, Cantley LC, Cerione RA, Carraway KL 3rd. Insect cell-expressed p180erbB3 possesses an impaired tyrosine kinase activity. Proc Natl Acad Sci USA. 1994; 91:8132–6. [PubMed: 8058768]
12. Shi F, Telesco SE, Liu Y, Radhakrishnan R, Lemmon MA. ErbB3/HER3 intracellular domain is competent to bind ATP and catalyze autophosphorylation. Proc Natl Acad Sci USA. 2010; 107:7692–7. [PubMed: 20351256]
13. Berger MB, Mendrola JM, Lemmon MA. ErbB3/HER3 does not homodimerize upon neuregulin binding at the cell surface. FEBS Lett. 2004; 569:332–6. [PubMed: 15225657]
14. Tzahar E, Waterman H, Chen X, Levkowitz G, Karunagaran D, Lavi S, et al. A hierarchical network of interreceptor interactions determines signal transduction by Neu differentiation factor/neuregulin and epidermal growth factor. Mol Cell Biol. 1996; 16:5276–87. [PubMed: 8816440]
15. Pinkas-Kramarski R, Soussan L, Waterman H, Levkowitz G, Alroy I, Klapper L, et al. Diversification of Neu differentiation factor and epidermal growth factor signaling by combinatorial receptor interactions. EMBO J. 1996; 15:2452–67. [PubMed: 8665853]
16. Wallasch C, Weiss FU, Niederfellner G, Jallal B, Issing W, Ullrich A. Heregulin-dependent regulation of HER2/neu oncogenic signaling by heterodimerization with HER3. EMBO J. 1995; 14:4267–75. [PubMed: 7556068]
17. Wilson TR, Lee DY, Berry L, Shames DS, Settleman J. Neuregulin-1-mediated autocrine signaling underlies sensitivity to HER2 kinase inhibitors in a subset of human cancers. Cancer Cell. 2011; 20:158–72. [PubMed: 21840482]

Author Manuscript Author Manuscript Author Manuscript Author Manuscript

18. Sheng Q, Liu X, Fleming E, Yuan K, Piao H, Chen J, et al. An activated ErbB3/NRG1 autocrine loop supports in vivo proliferation in ovarian cancer cells. Cancer Cell. 2010; 17:298–310. [PubMed: 20227043]
19. Yarden Y, Sliwkowski MX. Untangling the ErbB signalling network. Nat Rev Mol Cell Biol. 2001; 2:127–37. [PubMed: 11252954]
20. Buac K, Xu M, Cronin J, Weeraratna AT, Hewitt SM, Pavan WJ. NRG1 / ERBB3 signaling in melanocyte development and melanoma: inhibition of differentiation and promotion of proliferation. Pigment Cell Melanoma Res. 2009; 22:773–84. [PubMed: 19659570]
21. Reschke M, Mihic-Probst D, van der Horst EH, Knyazev P, Wild PJ, Hutterer M, et al. HER3 is a determinant for poor prognosis in melanoma. Clin Cancer Res. 2008; 14:5188–97. [PubMed: 18698037]
22. Tworkoski K, Singhal G, Szpakowski S, Zito CI, Bacchiocchi A, Muthusamy V, et al. Phosphoproteomic screen identifies potential therapeutic targets in melanoma. Mol Cancer Res. 2011; 9:801–12. [PubMed: 21521745]
23. Abel EV, Basile KJ, Kugel CH III, Witkiewicz AK, Le K, Amaravadi RK, et al. Melanoma adapts to RAF/MEK inhibitors by FOXD3-dependent upregulation of ERBB3 by FOXD3. J Clin Invest. 2013; 123:2155–68. [PubMed: 23543055]
24. Wich LG, Hamilton HK, Shapiro RL, Pavlick A, Berman RS, Polsky D, et al. Developing a multidisciplinary prospective melanoma biospecimen repository to advance translational research. Am J Trans Res. 2009; 1:35–43.
25. Gaborit N, Abdul-Hai A, Mancini M, Lindzen M, Lavi S, Leitner O, et al. Examination of HER3 targeting in cancer using monoclonal antibodies. Proc Natl Acad Sci USA. 2015; 112:839–44. [PubMed: 25564668]
26. Vasudevan KM, Barbie DA, Davies MA, Rabinovsky R, McNear CJ, Kim JJ, et al. AKT-independent signaling downstream of oncogenic PIK3CA mutations in human cancer. Cancer Cell. 2009; 16:21–32. [PubMed: 19573809]
27. Park ES, Rabinovsky R, Carey M, Hennessy BT, Agarwal R, Liu W, et al. Integrative analysis of proteomic signatures, mutations, and drug responsiveness in the NCI 60 cancer cell line set. Mol Cancer Therap. 2010; 9:257–67. [PubMed: 20124458]
28. Gopal YN, Deng W, Woodman SE, Komurov K, Ram P, Smith PD, et al. Basal and treatment-induced activation of AKT mediates resistance to cell death by AZD6244 (ARRY-142886) in Braf-mutant human cutaneous melanoma cells. Cancer Res. 2010; 70:8736–47. [PubMed: 20959481]
29. Kaplan FM, Kugel CH, Dadpey N, Shao Y, Abel EV, Aplin AE. SHOC2 and CRAF mediate ERK1/2 reactivation in mutant NRAS-mediated resistance to RAF inhibitor. J Biol Chem. 2012; 287:41797–807. [PubMed: 23076151]
30. Prickett TD, Agrawal NS, Wei X, Yates KE, Lin JC, Wunderlich JR, et al. Analysis of the tyrosine kinome in melanoma reveals recurrent mutations in ERBB4. Nat Genet. 2009; 41:1127–32. [PubMed: 19718025]
31. Setiady YY, Skaletskaya A, Coccia J, Moreland J, Carrigan C, Rui L, et al. huHER3-8, a novel humanized anti-HER3 antibody that inhibits exogeneous ligand-independent proliferation of tumor cells. Cancer Res. 2011; 71 Abstract nr 4564.
32. Sithanandam G, Anderson LM. The ERBB3 receptor in cancer and cancer gene therapy. Cancer Gene Ther. 2008; 15:413–48. [PubMed: 18404164]
33. Silva JM, Bulman C, McMahon M. BRAFV600E cooperates with PI3K signaling, independent of AKT, to regulate melanoma cell proliferation. Mol Cancer Res. 2014; 12:447–63. [PubMed: 24425783]
34. Kugel CH III, Hartsough EJ, Davies MA, Setiady YY, Aplin AE. Function-blocking ERBB3 antibody inhibits the adaptive response to RAF inhibitor. Cancer Res. 2014; 74:4122–32. [PubMed: 25035390]
35. Hoek KS, Eichhoff OM, Schlegel NC, Dobbeling U, Kobert N, Schaerer L, et al. In vivo switching of human melanoma cells between proliferative and invasive states. Cancer Res. 2008; 68:650–6. [PubMed: 18245463]

Author Manuscript Author Manuscript Author Manuscript Author Manuscript

36. Zhang K, Wong P, Zhang L, Jacobs B, Borden EC, Aster JC, et al. A Notch1-neuregulin1 autocrine signaling loop contributes to melanoma growth. Oncogene. 2012; 31:4609–18. [PubMed: 22249266]
37. Montero-Conde C, Ruiz-Llorente S, Dominguez JM, Knauf JA, Viale A, Sherman EJ, et al. Relief of feedback inhibition of HER3 transcription by RAF and MEK inhibitors attenuates their antitumor effects in BRAF-mutant thyroid carcinomas. Cancer Discov. 2013; 3:520–33. [PubMed: 23365119]
38. Mei L, Xiong WC. Neuregulin 1 in neural development, synaptic plasticity and schizophrenia. Nat Rev Neurosci. 2008; 9:437–52. [PubMed: 18478032]
39. Soltoff SP, Carraway KL 3rd, Prigent SA, Gullick WG, Cantley LC. ErbB3 is involved in activation of phosphatidylinositol 3-kinase by epidermal growth factor. Mol Cell Biol. 1994; 14:3550–8. [PubMed: 7515147]
40. Kim HH, Vijapurkar U, Hellyer NJ, Bravo D, Koland JG. Signal transduction by epidermal growth factor and heregulin via the kinase-deficient ErbB3 protein. Biochem J. 1998; 334:189–95. [PubMed: 9693119]
41. LoRusso P, Janne PA, Oliveira M, Rizvi N, Malburg L, Keedy V, et al. Phase I study of U3-1287, a fully human anti-HER3 monoclonal antibody, in patients with advanced solid tumors. Clin Cancer Res. 2013; 19:3078–87. [PubMed: 23591447]
42. Schoeberl B, Pace EA, Fitzgerald JB, Harms BD, Xu L, Nie L, et al. Therapeutically targeting ErbB3: a key node in ligand-induced activation of the ErbB receptor-PI3K axis. Sci Signal. 2009; 2:ra31. [PubMed: 19567914]
43. Garner AP, Bialucha CU, Sprague ER, Garrett JT, Sheng Q, Li S, et al. An antibody that locks HER3 in the inactive conformation inhibits tumor growth driven by HER2 or neuregulin. Cancer Res. 2013; 73:6024–35. [PubMed: 23928993]
44. Liu J, Ray-Coquard IL, Selle F, Poveda A, Cibula D, Hirte HW, et al. A phase II randomized open-label study of MM-121, a fully human monoclonal antibody targeting ErbB3, in combination with weekly paclitaxel versus weekly paclitaxel in patients with platinum-resistant/ refractory ovarian cancers. J Clin Oncol. 2014; 32(suppl):5519.
45. Sequist LV, Chavez A, Doebele RC, Gray JE, Harb WA, Modiano MR, et al. A randomized phase 2 trial of MM-121, a fully human monoclonal antibody targeting ErbB3, in combination with erlotinib in EGFR wild-type NSCLC patients. J Clin Oncol. 2014; 32(suppl):8051.
46. Higgins MJ, Doyle C, Paepke S, Azaro A, Martin M, Semiglazov V, et al. A randomized, double-blind phase II trial of exemestane plus MM-121 (a monoclonal antibody targeting ErbB3) or placebo in postmenopausal women with locally advanced or metastatic ER+/PR+, HER2-negative breast cancer. J Clin Oncol. 2014; 32(suppl):587. [PubMed: 24419113]
47. Baselga J, Cortes J, Kim SB, Im SA, Hegg R, Im YH, et al. Pertuzumab plus trastuzumab plus docetaxel for metastatic breast cancer. N Engl J Med. 2012; 366:109–19. [PubMed: 22149875]

Author Manuscript
Author Manuscript
Author Manuscript
Author Manuscript

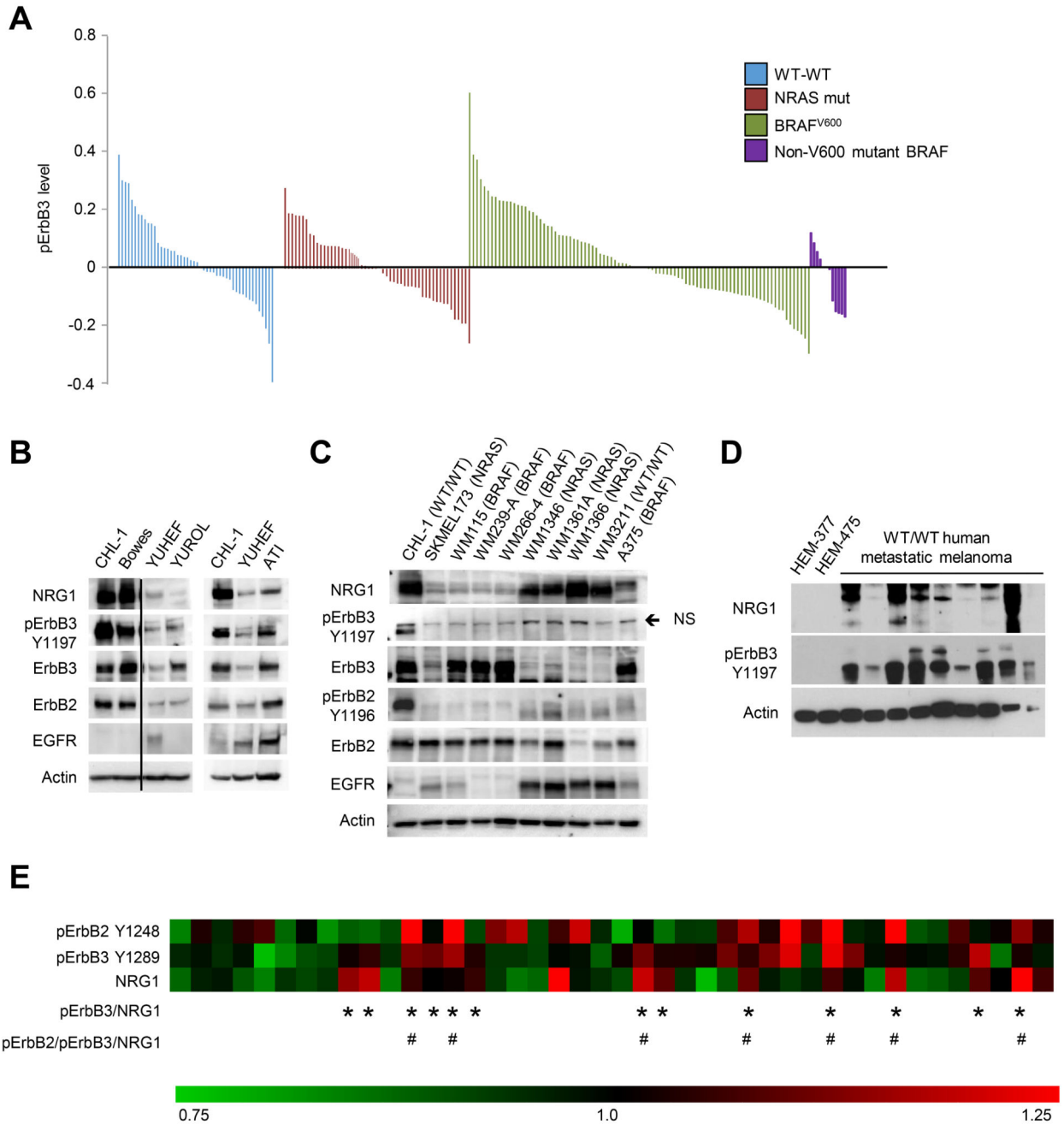

Figure 1. Elevated phospho-ErbB3 levels in a subset of WT/WT melanoma

A) Graph of relative levels of phospho-ErbB3 level in V600E/K BRAF, other mutant BRAF; mutant NRAS and WT/WT melanomas from TCGA RPPA data. Results are expressed as load-corrected log2 data on the y-axis. B) Lysates from WT/WT cell lines growing in normal conditions were analyzed by Western blotting for NRG1, phospho- and total ErbB3, phospho- and total ErbB2, EGFR and actin (loading control). C) WT/WT, mutant BRAF, and mutant NRAS cell lines were lysed and lysates analyzed by Western blotting with the antibodies indicated. The arrow in the phospho-ErbB3 blot indicates a non-

Author Manuscript Author Manuscript Author Manuscript Author Manuscript

specific (NS) band and was determined by knockdown experiments. D) Nine fresh-frozen metastatic WT/WT melanoma tumors from patients were micro-dissected, harvested and lysed in extraction buffer. Lysates were analyzed by Western blot for NRG1, phospho-ErbB3, and actin (loading control). Two melanocytes cell lines (HEM-377 and HEM-475) were used as a control. E) Heat map showing phospho-ErbB2, phospho-ErbB3 and NRG1 levels in WT/WT patient samples from the RPPA TCGA dataset. Data were normalized to the median value for each gene across all genotypes, and analyzed with MultiExperiment Viewer (MEV) program. Samples were normalized relative to median for the individual target. * represents patient samples co-expressing above median phospho-ErbB3 and NRG1. # represents patient samples co-expressing above median levels of phospho-ErbB2, phospho-ErbB3 and NRG1.

Author Manuscript Author Manuscript Author Manuscript Author Manuscript

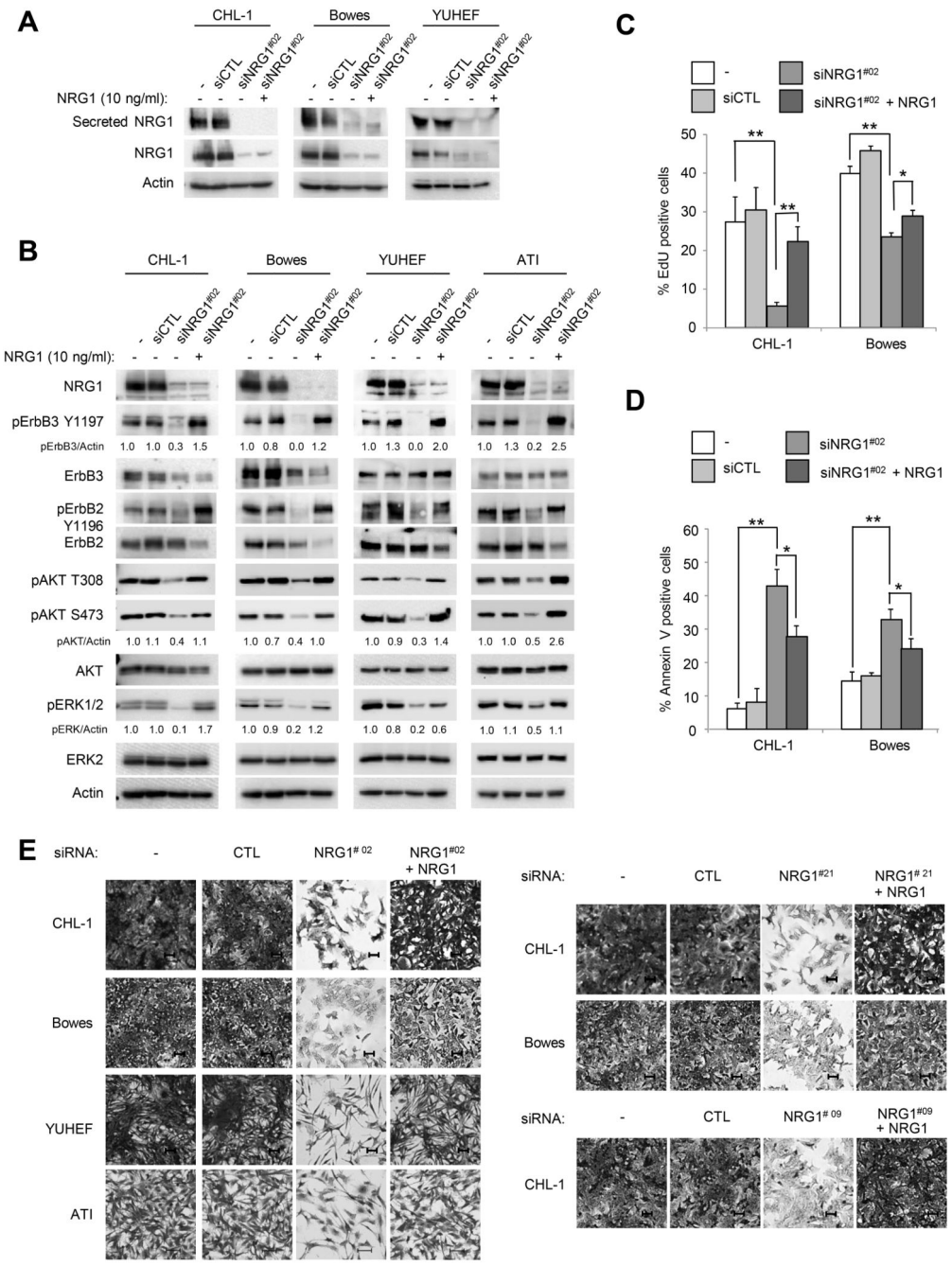

Figure 2. NRG1 is required for S-phase entry and survival in WT/WT melanoma cells

A) CHL-1, Bowes and YUHEF cells were treated with reagent alone (-), transfected with a non-targeting control siRNA (CTL) or transfected with NRG1-targeting siRNA (#02) for 72 hr. An additional NRG1 siRNA transfection was performed in the presence of exogenous NRG1 (10 ng/ml). Medium was changed to serum free for the final 24 hr (maintaining exogenous NRG1 in one condition). Media and cell lysates were analyzed by Western blotting with the antibodies indicated. B) CHL-1, Bowes, YUHEF and ATI cells were transfected similar to A). Media and NRG1 were replaced after 48 hr. Cells were lysed and

Author Manuscript Author Manuscript Author Manuscript Author Manuscript

lysates analyzed by Western blotting with the antibodies indicated. C) Cells were transfected with CTL or NRG1 #02 siRNAs, as above. After 72 hr, cells were incubated with EdU for 5 hr and then analyzed for EdU incorporation by FACS analysis. The results are the mean −/+ SD of three independent experiments. *P<0.05, **P<0.01. D) CHL-1 and Bowes cells were transfected similar to A). After 72 hr, cells were replated in 3D collagen gels and, after further 48 hr, annexin V staining was performed. The results are the mean −/+ SD of three independent experiments. *P<0.05, **P<0.01. E) CHL-1, Bowes, YUHEF and ATI cells were transfected with CTL or with different NRG1 siRNAs (#02, #21, #09) −/+ exogenous NRG1 (10 ng/ml). After 3 days, cells were replated for a further 96 hr before fixation. Fixed cells were stained with crystal violet and pictures taken with 20× magnification. Scale bars represent 50 μm.

Author Manuscript
Author Manuscript
Author Manuscript
Author Manuscript

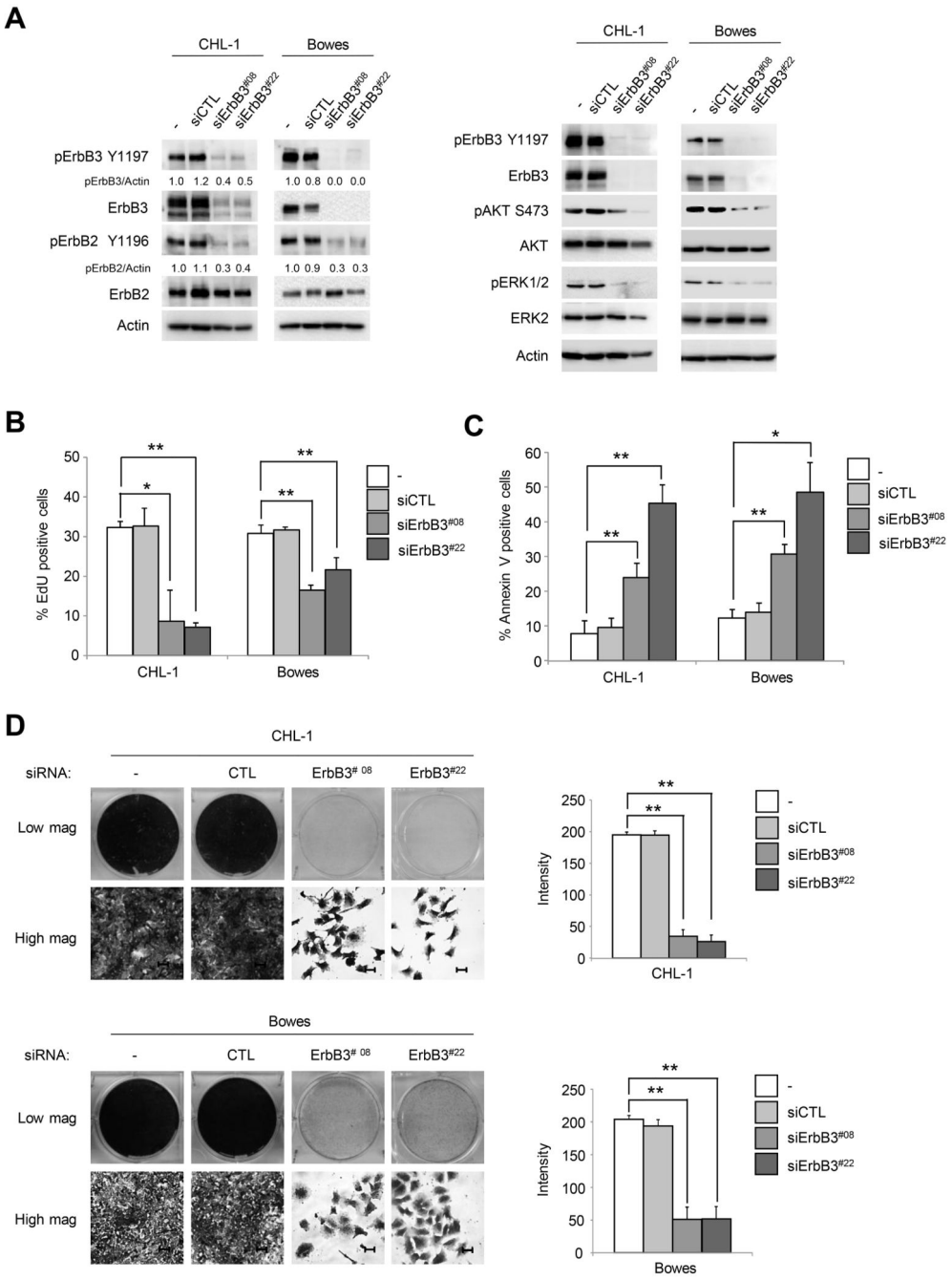

Figure 3. Depletion of ErbB3 reduces S-phase entry and cell growth and induces apoptosis

A) CHL-1 and Bowes cells were treated with reagent alone (-), transfected with a control siRNA (CTL), or transfected with one of two distinct ErbB3-targeting siRNA for 72 hr. Cells lysates were analyzed by Western blotting. B) CHL-1 and Bowes cells were treated as in A) and incubated with EdU for 5 hr before analysis for S-phase entry by FACS. Shown is the mean −/+ SD from three independent experiments. *P<0.05, **P<0.01. C) CHL-1 and Bowes cells were transfected similar to A). After 72 hr, cells were replated in 3D collagen and annexin V staining was performed after further 48 hr. The results are the mean −/+ SD

Author Manuscript Author Manuscript Author Manuscript Author Manuscript

of three independent experiments. *P<0.05, **P<0.01. D) Cells were transfected similar to A). After 3 days cells were replated for a further 96 hr before fixation. Fixed cells were stained with crystal violet and pictures taken with 20× magnification. Crystal violet quantification was performed using Image J. *P<0.05, **P<0.01. Scale bars represent 50 μm. Graphed is the mean intensity from three independent samples assayed in parallel.

Author Manuscript Author Manuscript Author Manuscript Author Manuscript

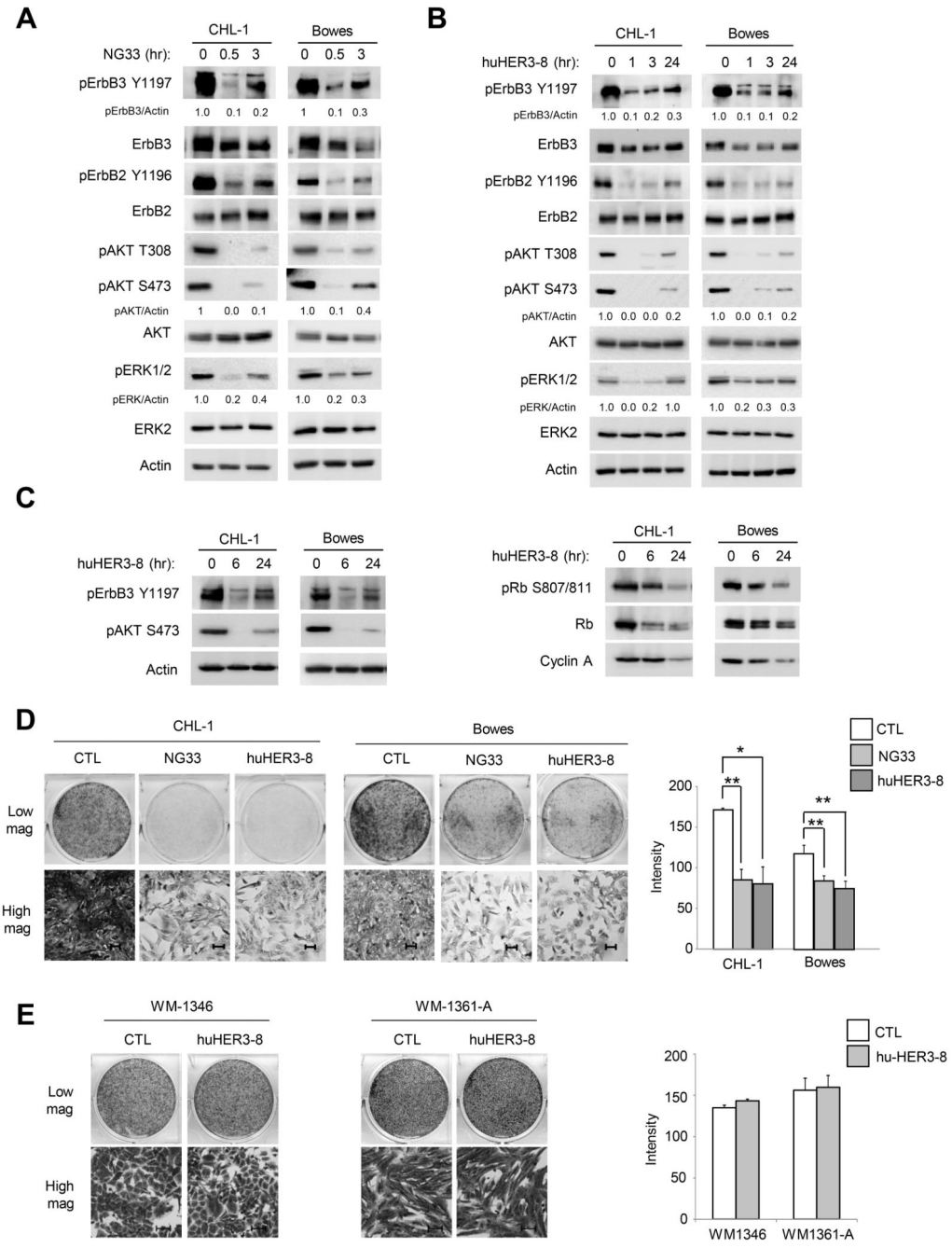

Figure 4. Targeting ErbB3 with neutralizing antibodies reduces phosphorylation of AKT and ERK1/2 and inhibits cell growth

A) CHL-1 and Bowes were treated individually with the ErbB3 antibody, NG33 (10 μg/ml) for 30 min or 3 hr. Cells were lysed and lysates Western blotted, as indicated. B) As in A), except cells were treated with huHER3-8 (10 μg/ml) for 1, 3 or 24 hr. C) CHL-1 and Bowes were treated with huHER3-8 (10 μg/ml) for 6 or 24 hr. Cells lysates were Western blotted, as indicated. D) CHL-1 and Bowes cells were plated at low density and the next day treated with either NG33 (10 μg/ml) or with huHER3-8 (10 μg/ml). Medium containing antibodies were replaced after 72 hr. After 6 days, cells were fixed and stained with crystal violet;

Author Manuscript Author Manuscript Author Manuscript Author Manuscript

pictures were taken with 20× magnification. Image J was used for crystal violet quantification. *P<0.05, **P<0.01. Scale bars represent 50 μm. Graphed is the mean intensity from 3 independent experiments. E) WM1346 and WM1361A cells were plated at low density and the next day treated with huHER3-8 (10 μg/ml). Medium containing huHER3-8 was replaced after 72 hr. After 6 days, cells were fixed and stained with crystal violet; pictures were taken with 20× magnification. Scale bars represent 50 μm. Graphed is the mean intensity from 3 independent experiments.

Author Manuscript
Author Manuscript
Author Manuscript
Author Manuscript

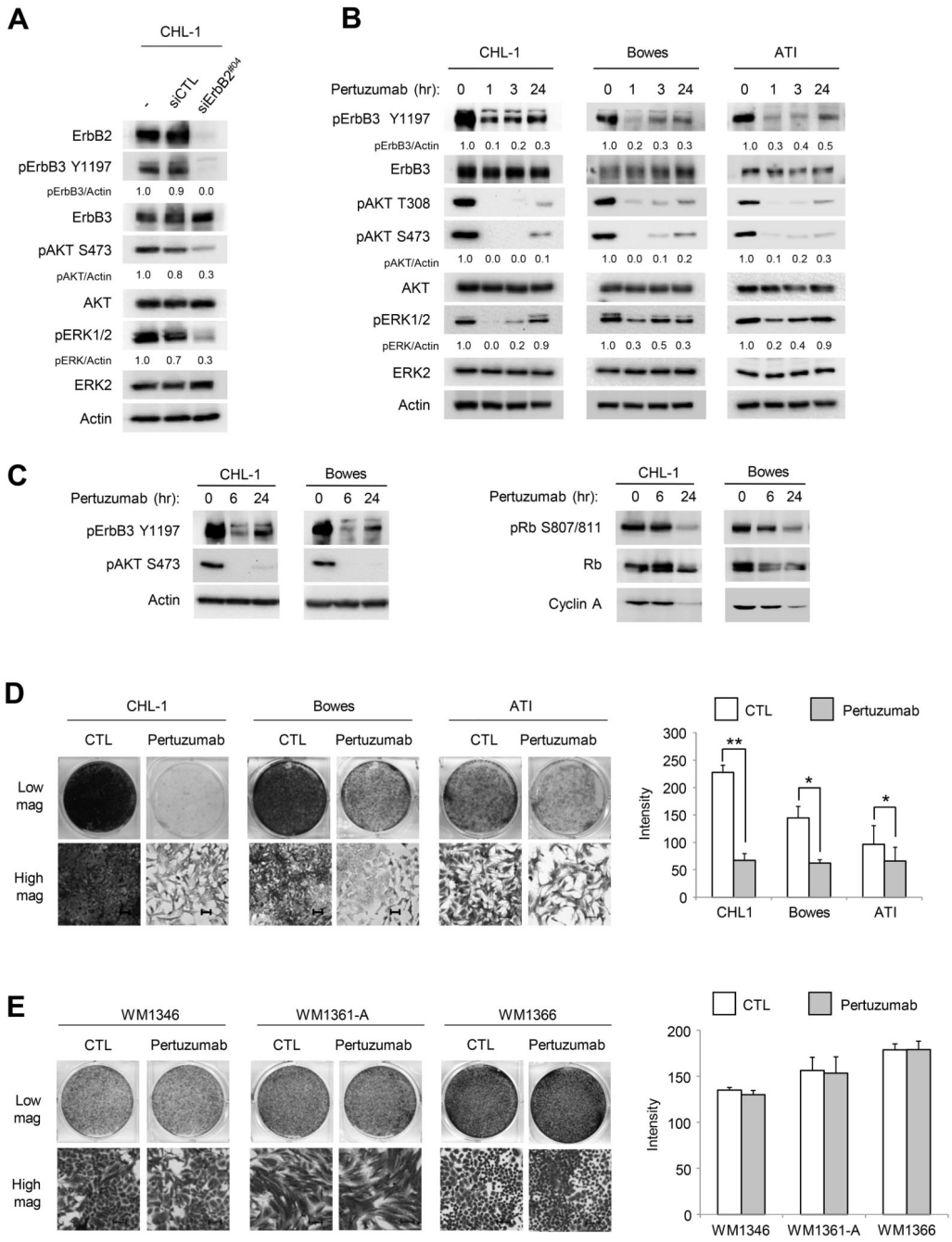

Figure 5. Targeting ErbB2 reduces phosphorylation of AKT and ERK1/2 and inhibits cell growth *in vitro*

A) CHL-1 cells were treated with reagent alone (-), transfected with a control siRNA (CTL), or transfected with ErbB2-targeting siRNA for 72 hr. Cell lysates were Western blotted, as indicated. B) CHL-1, Bowes and ATI cells were treated with pertuzumab (1 μg/ml) for 1, 3 or 24 hr. Cells lysates were Western blotted, as indicated. C) CHL-1 and Bowes cells were treated with pertuzumab (1 μg/ml) for 6 or 24 hr. Cells lysates were Western blotted, as indicated. D) CHL-1, Bowes and ATI cells were plated at clonal density and on the next day treated with pertuzumab (1 μg/ml). Medium and treatments were replaced every 3 days.

Author Manuscript Author Manuscript Author Manuscript Author Manuscript

After 6 days of treatment for CHL-1 and Bowes and 10 days of treatment for ATI, cells were fixed and stained with crystal violet. Cell pictures were taken with 20× magnification. Crystal violet quantification was performed using Image J. *P<0.05, **P<0.01. Scale bars represent 50 μm. Graphed is the mean intensity from 3 independent experiments. E) WM1346, WM1361A and WM1366 cells were plated at low density and treated similar to D). Medium and treatments were replaced after 3 days. After a further 3 days, cells were fixed and stained with crystal violet. Crystal violet quantification was performed using Image J. Scale bars represent 50 μm. Graphed is the mean intensity from 3 independent experiments.

Author Manuscript Author Manuscript Author Manuscript Author Manuscript

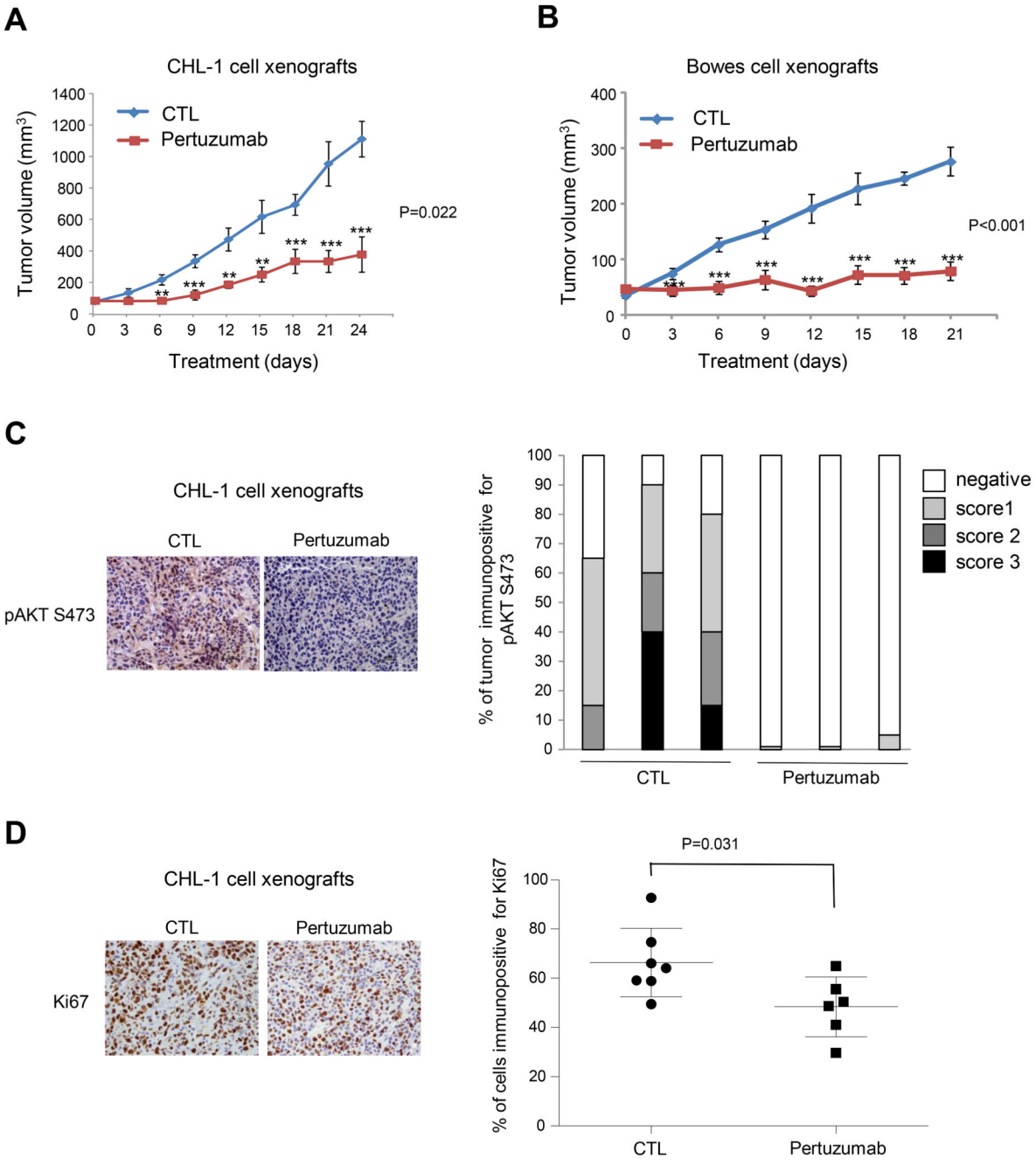

Figure 6. Pertuzumab inhibits tumor growth and reduces phosphorylation of AKT *in vivo*

A) Graph representing tumor volume −/+ SEM in CHL-1 xenografts (n=8 per condition) in nude mice treated intraperitoneally either with vehicle or pertuzumab (200 μg/mouse) every 3 days. **P<0.01, ***P<0.001. The difference between tumor growth rates (population average slopes of time trends in log-transformed tumor volumes) of the pertuzumab and control groups was statistically significant (P=0.022). B) Graph representing tumor volume −/+ SEM in Bowes xenografts (n=8 per condition) in nude mice treated intraperitoneally either with vehicle or pertuzumab every 3 days. ***P<0.001. The difference between tumor

Author Manuscript Author Manuscript Author Manuscript Author Manuscript

growth rates of the pertuzumab and control groups was statistically significant (P<0.001). C) Representative images and quantification of CHL-1 control and pertuzumab-treated xenografts analyzed by IHC for pS473 AKT. Magnification 400×. D) Representative images and scatter plot graph quantification of CHL-1 control and pertuzumab-treated xenografts analyzed by IHC for Ki67. Magnification 400×. The difference between the percentage of Ki67-positive cells between pertuzumab-treated and the control tumors was statistically significant (P=0.0314).

Author Manuscript Author Manuscript Author Manuscript Author Manuscript

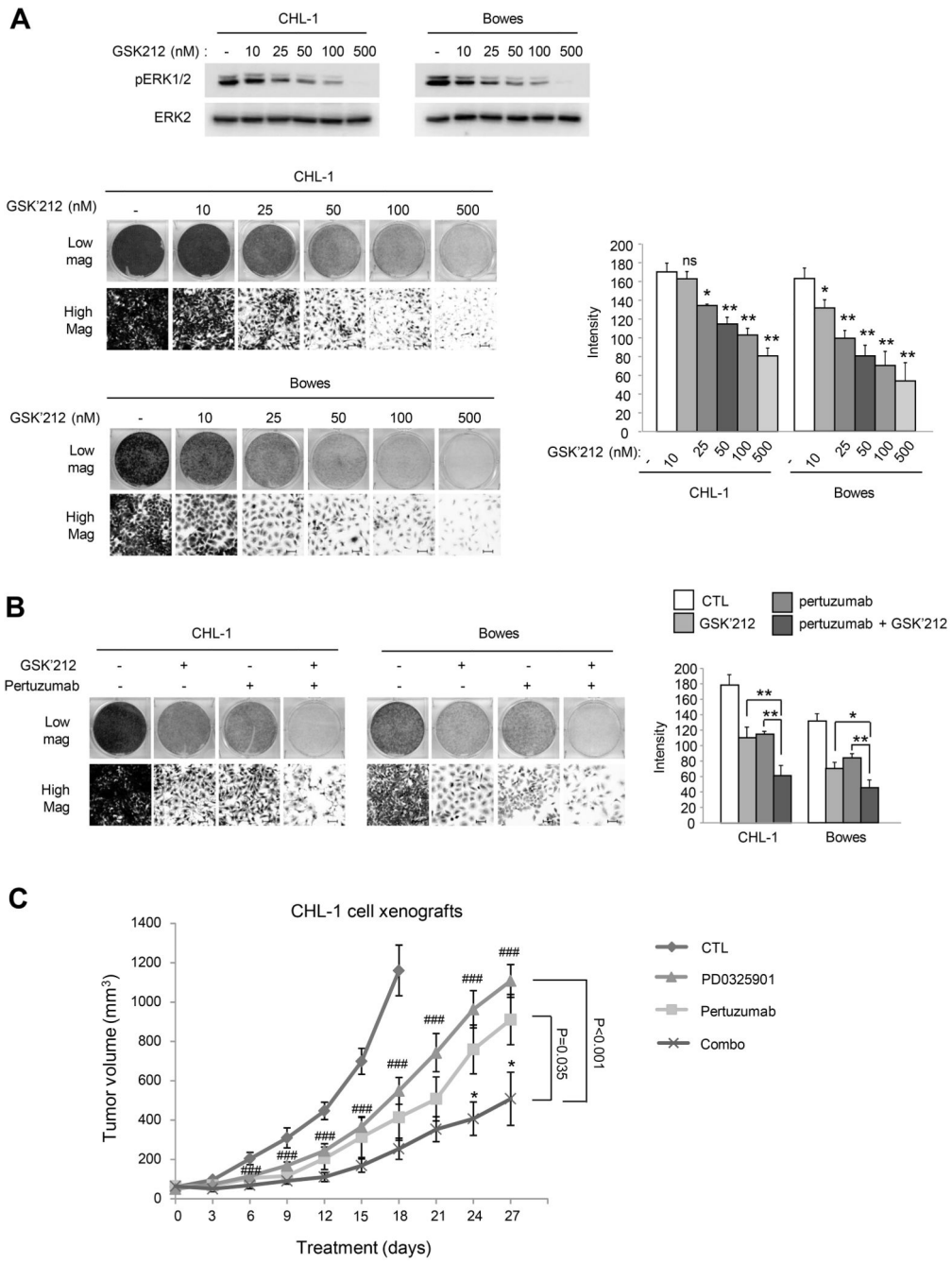

Figure 7. Pertuzumab increases MEK inhibitor efficacy *in vitro* and *in vivo* in WT/WT melanoma

A) CHL1 and Bowes cells were treated for 48 hr with increasing concentrations of GSK'212 (10, 25, 50, 100 and 500 nM). Cells were lysed and lysates Western blotted, as indicated (upper panel). Cells were plated at clonal density and treated as indicated. Medium and GSK'212 were replaced after 3 days. After 6 days cells were fixed and stained with crystal violet (lower panel). Crystal violet was quantified using Image J. *P<0.05, **P<0.01. Scale bars represent 50 μm. Graphed is the mean intensity from 3 independent experiments. B) Cells were treated with GSK'212 (50 nM) alone, pertuzumab (1 μg/ml) alone or in

Author Manuscript Author Manuscript Author Manuscript Author Manuscript

combination. Medium and treatments were replaced after 3 days. After a further 3 days, cells were fixed and stained with crystal violet. *P<0.05, **P<0.01. Scale bars represent 50 μm. Graphed is the mean intensity from 3 independent experiments. C) Graph representing average tumor volume −/+ SEM in CHL-1 xenografts in nude mice treated either with vehicle, pertuzumab alone (200 μg/mouse), MEK inhibitor alone (PD0325901 chow at 7 mg/kg), or pertuzumab in combination with PD0325901 (combo); pertuzumab was administered intraperitoneally every 3 days. *P<0.05, pertuzumab alone vs combo; ###P<0.001 MEK inhibitor alone vs combo.